Thermotropic and Mixing Behavior of Mixed-Chain Phosphatidylcholines with Molecular Weights Identical with That of L-α-Dipalmitoylphosphatidylcholine†

Thomas Bultmann,‡ Hai-nan Lin, Zhao-qing Wang, and Ching-hsien Huang*
Department of Biochemistry, Health Sciences Center, University of Virginia, Charlottesville, Virginia 22908
Received January 18, 1991; Revised Manuscript Received April 16, 1991

ABSTRACT: The thermotropic phase behavior of 10 mixed-chain phosphatidylcholines, in excess water, has been examined and compared with that of identical-chain C(16):C(16)PC by using high-resolution differential scanning calorimetry (DSC). The molecular weights (MW) of these 11 molecular species are the same, but their $\Delta C/CL$ values, or the normalized chain length differences, vary considerably, ranging from 0.035 to 0.540. The thermodynamic parameters (T_m, ΔH, and ΔS) associated with the main phase transitions for these lipid dispersions exhibit biphasic V-shaped curves, when plotted against $\Delta C/CL$. Similar characteric curves have been reported previously for aqueous dispersions of mixed-chain phosphatidylcholines with MW identical with that of C(17):C(17)PC [Lin et al. (1990) *Biochemistry 29*, 7063–7072]. The initial decrease in T_m (ΔH or ΔS) with increasing values of $\Delta C/CL$ is attributed to the progressive increase in the magnitude of the chain-terminal perturbations on the conformational statistics of the adjacent hydrocarbon chains and hence the lateral chain–chain contact interactions of these mixed-chain phosphatidylcholines in the gel-state bilayer. At $\Delta C/CL \cong 0.42$, the chain-end perturbation is presumably at its maximum; beyond this point, the highly asymmetric phosphatidylcholines are proposed to pack, at $T < T_m$, into the mixed interdigitated bilayer. In this new packing mode, the methyl ends of the longer acyl chains are relocated at the interfaces between the hydrocarbon core of the bilayer and the aqueous medium. This disposition of the bulky chain ends releases a certain degree of chain–chain packing disorders, leading to an increase in T_m (ΔH or ΔS) with increasing $\Delta C/CL$. The mixing behavior of C(12):C(20)PC/C(16):C(16)PC, C(20):C(12)PC/C(10):C(22)PC, and C(10):C(22)PC/C(16):C(16)PC binary lipid systems is also studied. The results, in terms of the phase diagram, support the molecular interpretations given for the biphasic V-shaped curve observed in the T_m (ΔH or ΔS) vs $\Delta C/CL$ plot.

Recently, we have made extensive use of high-resolution differential scanning calorimetry (DSC)[1] to examine the thermotropic phase behavior of various mixed-chain phosphatidylcholines in excess water (Huang & Mason, 1986; Huang, 1990). In studying aqueous dispersions prepared from a series of phosphatidylcholines with molecular weight (MW) identical with that of C(17):C(17)PC, the thermodynamic parameters associated with the main phase transitions (T_m, ΔH, and ΔS) of these lipid dispersions were found to exhibit a biphasic behavior when plotted as a function of $\Delta C/CL$ (Huang, 1990; Lin et al., 1990). The structural parameter $\Delta C/CL$ is defined as the normalized chain-length difference between the two acyl chains within a given phosphatidylcholine molecule in the gel-state bilayer (Mason et al., 1981), and the value of $\Delta C/CL$ can be readily calculated based on the known structural formula of the phosphatidylcholine molecule (Huang, 1991). Specifically, the term ΔC is the effective chain-length difference between the *sn*-1 and *sn*-2 acyl chains, in C–C bond lengths, and the other term CL is defined as the effective length of the longer of the two acyl chains, also in C–C bond lengths. In calculation of the values of ΔC and CL, an inherent shortening of 1.5 C–C bond lengths for the *sn*-2 acyl chain should always be taken into account, since the conformational disparity between the *sn*-1 and *sn*-2 acyl chains appears to be a fundamental feature for phosphatidylcholines in the gel-state bilayer (Yeagle, 1987).

In the T_m (ΔH or ΔS) versus $\Delta C/CL$ plot, the value of T_m (ΔH or ΔS) is observed to decrease initially with increasing values of $\Delta C/CL$, and as the value of $\Delta C/CL$ exceeds 0.40 a reverse trend is observed, resulting in a biphasic V-shaped curve (Huang, 1990; Lin et al., 1990). The position of the minimum at about $\Delta C/CL = 0.40$ corresponds to the structural parameter of C(20):C(14)PC, reflecting that highly asymmetric phosphatidylcholines with $\Delta C/CL > 0.4$ such as C(22):C(12)PC and less asymmetric phosphatidylcholines with $\Delta C/CL < 0.4$ such as C(17):C(17)PC can self-assemble in excess water into the mixed interdigitated and partially interdigitated bilayers, respectively, at $T < T_m$ (Huang, 1990; Lin et al., 1990). In accord with the proposed acyl chain packings at $T < T_m$ is the eutectic mixing behavior of C(22):C(12)PC/C(17):C(17)PC, demonstrating extended regions of gel–gel phase separation of the binary mixtures in the two-dimensional plane of the lipid bilayer (Sisk et al., 1990).

Saturated identical-chain C(16):C(16)PC is perhaps one of the most widely studied phospholipids. Upon being heated in the temperature range of 5–60 °C, fully hydrated C(16):C(16)PC lamellae undergo multiple phase transitions at the atmospheric pressure, and the transition scheme is well characterized as follows: $L_c \rightarrow L_{\beta'} \rightarrow P_{\beta'} \rightarrow L_\alpha$, where L_c, $L_{\beta'}$, $P_{\beta'}$, and L_α are the crystalline or subgel phase, tilted gel phase, rippled gel phase, and liquid-crytalline or fluid phase, re-

† This research was supported by NIH Grant GM-17452. This study made use of a Hart 7708 calorimeter, which was purchased with funds provided, in part, by Instrumentation Grant Dir-8907318 from National Science Foundation.
* To whom correspondence should be addressed.
‡ Present address: Department of Spectroscopy, Max-Planck-Institute for Biophysical Chemistry, D-3400, Goettingen, Germany.

[1] Abbreviations: C(X):C(Y)PC, saturated L-α-phosphatidylcholine having X carbons in the *sn*-1 acyl chain and Y carbons in the *sn*-2 acyl chain; DSC, differential scanning calorimetry; MW, molecular weight; T_m, the main phase-transition temperature.

0006-2960/91/0430-7194$02.50/0

spectively (Chapman et al., 1967; Chen et al., 1980; Ruocco & Shipley, 1982). In the presence of increasing concentrations of ethanol, the T_m value of fully hydrated C(16):C(16)PC lamellae exhibits a biphasic behavior (Rowe, 1983). This biphasic effect of ethanol has been attributed to the transformation of gel-state C(16):C(16)PC lamellae into the fully interdigitated phase (Simon & McIntosh, 1984; Nambi et al., 1988; Ohki et al., 1990). In fact, fully hydrated C(16):C(16)PC lamellae can be induced, at $T < T_m$, by many chemical agents and also under high pressure to undergo the gel phase to the fully interdigitated phase transition (Simon et al., 1986; Slater & Huang, 1988). It is thus of great interest to obtain thermodynamic information for aqueous dispersions of those mixed-chain phosphatidylcholines whose properties can be correlated to or compared with those of C(16):C(16)PC dispersions. Consequently, we have extended our previous DSC studies to investigate the thermotropic phase behavior of aqueous lipid dispersions prepared from a series of mixed-chain phosphatidylcholines with MW identical with that of C(16):C(16)PC. In addition, in the present work we have investigated the mixing behavior of C(16):C(16)PC/C(10):C(22)PC, C(16):C(16)PC/C(12):C(20)PC, and C(20):C(12)PC/C(10):C(22)PC binary mixtures by high-resolution DSC.

Materials and Methods

Fatty acids and lysophosphatidylcholines with various acyl chain lengths were purchased from Sigma (St. Louis, MO) and Avanti Polar Lipids, Inc. (Birmingham, AL), respectively. Silica gel 60 (mesh number: 230–400) was provided by EM Science (Gibbstown, NJ). Other reagents and organic solvents were reagent grade and spectroscopic grade, respectively.

Mixed-chain phosphatidylcholines were synthesized at room temperature by acylation of $CdCl_2$ adducts of lysophosphatidylcholine, in dry chloroform, with fatty acid anhydride in the presence of catalyst 4-pyrrolidinopyridine, and were purified by column chromatography on silica gel. The detailed procedures used for the synthesis and purification were the same as those previously employed in this laboratory (Lin et al., 1990).

The thermotropic phase behavior of aqueous dispersions of pure one-component phospholipid was studied with a high-resolution MC-2 differential scanning calorimeter with cooling capability (Microcal Inc., Northampton, MA). For binary lipid mixtures, a Hart 7708 differential scanning calorimeter was also used (Hart Scientific, Pleasant Grove, UT). The samples for DSC experiments were prepared as described elsewhere (Lin et al., 1990; Lin & Huang, 1988). Prior to DSC experiments, the annealed samples were stored in cold room (0 °C) for a minimum of a week, if not specified in the figure legend. Each sample was scanned at least four times, two heating (scan rates of 10–15 °C/h) and two cooling (scan rates of 5–15 °C/h) runs. The concentrations of the lipid samples used for DSC experiments are usually in the range of 3–7 mM (MC-2 calorimeter) or about 20 mM (Hart calorimeter). It should be emphasized that in preparing aqueous dispersions of binary lipid mixtures, the binary lipid mixtures were subject to chloroform treatment in order to form homogeneous mixture prior to addition of aqueous buffer, following the established method 4 of Lin & Huang (1988). Because of the chloroform step, the T_m values of the aqueous sample may be shifted for some lipids. This shift is not caused by the presence of trace amounts of chloroform, since after the chloroform step the lipid has been extensively lyophilized. In the case of C(10):C(22)PC, we noticed an up-shift of about 2.8 °C in T_m. However, this up-shift in T_m did not affect the shape of the phase diagram to be constructed.

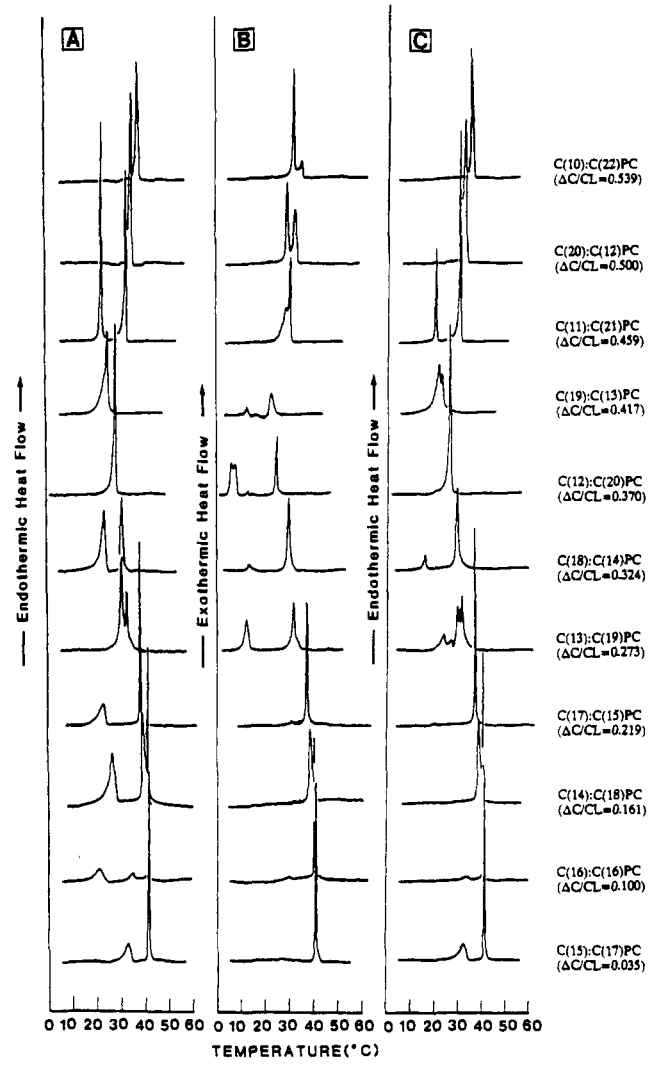

FIGURE 1: DSC profiles of various phosphatidylcholines, in excess water, with indicated values of $\Delta C/CL$. (A) The initial heating scans. (B) The first cooling scans. (C) Immediate reheating scans. Prior to the DSC scans, the preincubation times at 0 °C for the various samples, from the bottom to the top, are 8 days, 15 months, 4 days, 100 days, 5 days, 12 h, 3 days, 3 days, 2 days, 6 days, and 2 days, respectively.

Results

The Thermotropic Phase Behavior of Pure Single-Component Phospholipid Systems. The first DSC heating, subsequent cooling, and immediate reheating thermograms for aqueous dispersions prepared from 10 mixed-chain phosphatidylcholines and identical-chain C(16):C(16)PC are illustrated in Figure 1, panels A, B, and C, respectively. These 11 molecular species of saturated diacylphosphatidylcholines have a common MW of 734.1, but they are different in terms of the structural parameter $\Delta C/CL$. The values of $\Delta C/CL$ for these phospholipids are indicated in Figure 1, in which the DSC thermograms are arranged in the order of increasing value of $\Delta C/CL$, i.e., in the order of increasing asymmetry of lipid acyl chains. The bottommost thermograms were obtained with C(15):C(17)PC ($\Delta C/CL$ = 0.035), whose two parallel segments of the *sn*-1 and *sn*-2 acyl chains are nearly identical in length, and the uppermost thermograms were recorded for C(10):C(22)PC ($\Delta C/CL$ = 0.539), whose *sn*-1 acyl chain in an all-trans configuration is about half as long as the effective chain length of the *sn*-2 acyl chains.

It is evident that some of the phosphatidylcholine dispersions under study exhibit multiple phase transitions. On the basis

of DSC data alone, complete assignments of all these multiple phase transitions, particularly those displayed by C(13):C(19)PC in the second DSC heating thermogram, cannot be achieved unambiguously in relation to the various known bilayer phases. Nevertheless, applications of the thermal history dependency phenomena of the subtransition and pretransition, as presented below, permit partial assignments of some of the phase transitions depicted in Figure 1. The subtransition characteristics of C(16):C(16)PC depend most heavily on the thermal history of the sample (Chen et al., 1980; Ruocco & Shipley, 1982); in fact, the subtransition peak is usually abolished upon cooling or immediate reheating due to the extremely slow kinetics of the headgroup dehydration (Wu et al., 1985). The pretransition characteristics of C(16):C(16)PC lamellae are also known to depend on the thermal history, resulting in the temperature hysteresis phenomena (Lentz et al., 1978; Cho et al., 1981; Akiyama et al., 1982). The pretransition peak at 35.0 °C observed for C(16):C(16)PC lamellae in the first DSC heating scan is down-shifted by about 5 °C in the subsequent cooling scan (Figure 1A,B). On immediate reheating, the pretransition peak shifts upward to 34 °C, in between the pretransition temperatures observed in the first heating and first cooling curves (Figure 1C). In contrast, the transition characteristics associated with the main phase transition of C(16):C(16)PC dispersions are virtually independent of the thermal history of the lipid sample, indicating that the transition behavior of the main phase transition is practically reversible in all heating and cooling scans. In the case of mixed interdigitated bilayer systems such as C(18):C(10)PC and C(8):C(18)PC, the main phase transition is also known to be virtually completely reversible in all DSC heating scans; however, the T_m and ΔH values can be reduced significantly on cooling (Xu & Huang, 1987; Mattai et al., 1987; Chong & Choate, 1989; Shah et al., 1990). Nevertheless, the main phase transition of the bilayer, irrespect of the chain interdigitations, can be distinguished calorimetrically from the subtransition and pretransition based on the practically completely reversible behavior of the transition feature upon repeated heatings.

With the calorimetric criteria given above, some of the multiple phase transitions exhibited by the various lipid dispersions shown in Figure 1 can be assigned unequivocally. For instance, a large endothermic transition at 23.8 °C with ΔH = 8.5 kcal/mol is observed in Figure 1A for the sample of C(18):C(14)PC; however, this large transition is completely abolished on subsequent cooling (Figure 1B) and immediate reheating (Figure 1C). This transition at 23.8 °C can thus be assigned as the subtransition. A small transition occurring at 14.5 °C (ΔH = 0.6 kcal/mol) is also observed in Figure 1B for the same sample of C(18):C(14)PC; this transition shifts upward by 3.2 °C (ΔH = 0.9 kcal/mol) in Figure 1C upon immediate reheating. This small transition can thus be assigned as the pretransition due to the temperature hysteresis phenomena. The large high-temperature transition with T_m = 31.4 °C (ΔH = 6.6 kcal/mol) exhibited by the C(18):C(14)PC dispersion is virtually unchanged in all the three DSC curves shown in Figure 1A,B,C; consequently, it is assigned as the gel to liquid-crystalline phase transition or the main phase transition. It should be mentioned that our assignments for the various transition peaks of lamellar C(18):C(14)PC, in excess water, made on the basis of calorimetric criteria alone are in complete accord with the previous assignments put forward from the combined elegant X-ray and DSC studies of Mattai et al. (1987).

The subtransitions for dispersions of C(15):C(17)PC, C(16):C(16)PC, C(14):C(18)PC, C(17):C(15)PC, C(13):C(19)PC, C(18):C(14)PC, C(19):C(13)PC, and C(11):C(21)PC were assigned on the basis of their irreversible calorimetric behavior shown in Figure 1, to occur at 33.0, 19.6, 26.5, 20.6, 30.5, 23.8, 24.9, and 22.3 °C, respectively. Unlike C(16):C(16)PC, the subtransition endotherms for samples of C(15):C(17)PC and C(11):C(21)PC can be readily detected after incubations of the respective samples at low temperatures (≤5 °C) for 60 min. It is particularly noteworthy that an asymmetric endotherm in Figure 1A for the sample of C(19):C(13)PC can be identified. Upon cooling and reheating (Figure 1B,C), it becomes clear that the low-temperature shoulder of the asymmetric transition at 23.8 °C, observed in Figure 1A, is the main phase transition, whereas the sharp peak of the asymmetric transition at 24.9 °C is the subtransition. In this interesting case, the subtransition is observed to take place immediately after the main phase transition upon heating. An analogous thermal behavior has been previously observed for C(12):C(12)PC dispersions as reported first by Mabrey and Sturtevant (1976). The pretransitions, which could be more readily detected in the expanded DSC thermograms, for samples of C(16):C(16)PC, C(18):C(14)PC, and C(19):C(13)PC were assigned to occur at 35.0, 14.5, and 13.8 °C, respectively. Since the transition behavior of the subtransition depends heavily on the thermal history of the lipid sample and since the transition characteristics of the pretransitions are prone to marked temperature hysteresis, no attempt is thus made to compare the transition properties associated with the subtransition and pretransition for these various phospholipids because of their different thermal history as described in the legend to Figure 1.

The main phase transitions for all the lipid dispersions shown in Figure 1 were assigned on the basis of the reversible feature of the endotherm observed in the repeated DSC heating scans. The results, together with reported values in the literature, are summarized in Table I. The values of T_m associated with the main phase transitions for these lipid samples are plotted in Figure 2 against $\Delta C/CL$, resulting in a biphasic V-shaped curve. In this figure, the value of T_m is observed initially to decrease steadily with increasing values of $\Delta C/CL$; however, a point is reached beyond which the T_m value increases with increasing values of $\Delta C/CL$. This point of minimal value of T_m corresponds to the $\Delta C/CL$ value of 0.42 for C(19):C(13)PC. Interestingly, this curve observed in the T_m versus $\Delta C/CL$ plot is remarkably similar in shape to the curve connecting all the experimental T_m values for a series of saturated diacylphosphatidylcholines with identical MW of 762.2 including C(17):C(17)PC (Lin et al., 1990) as shown by the dashed line in Figure 2, raising the possibility of a general relationship between the structural parameter and the T_m for the lipid bilayer. Moreover, when the ΔH or ΔS values presented in Table I are plotted against $\Delta C/CL$, a V-shaped curve can also be obtained with the minimum value of ΔH (or ΔS) occurring near the $\Delta C/CL$ value of 0.42.

In assigning the main phase transition for C(12):C(20)PC dispersions, it is noted that the C(12):C(20)PC sample exhibits rather complex phase behavior upon cooling, although a distinct high-temperature exotherm peaked at 25.8 °C is clearly seen (Figure 1B). When scanned repeatedly in the ascending temperature mode from 2 to 45 °C, the phase behavior of C(12):C(20)PC is simple and reversible, as evidenced by the sharp single endotherm peaked at 28.1 °C with ΔH = 12.2 kcal/mol (Figure 1A,C). However, this simple endothermic transition shifts downward in temperature by 2.5 °C with a

Table I: Thermodynamic Parameters Associated with the Main Phase Transitions of Fully Hydrated Mixed-Chain Phosphatidylcholines with a Common MW Identical with That of C(16):C(16)PC

phospholipid	$\Delta C/CL$	T_m (°C)	ΔH (kcal/mol)	ΔS (cal mol^{-1} K^{-1})
C(15):C(17)PC[a]	0.035	41.7	10.1	34.9
C(16):C(16)PC[b]	0.100	41.4	8.74	27.8
C(16):C(16)PC[a]	0.100	41.5	8.5	27.0
C(14):C(18)PC[a]	0.161	39.2	8.8	28.2
C(14):C(18)PC[c]	0.161	38.6	6.9	22.2
C(14):C(18)PC[d]	0.161	42.0	8.2	26.0
C(14):C(18)PC[e]	0.161	38.2	7.9	25.4
C(14):C(18)PC[f]	0.161	39.3	7.9	25.3
C(17):C(15)PC[a]	0.219	37.7	7.4	23.8
C(13):C(19)PC[a]	0.271	32.6	7.2	23.5
C(13):C(19)PC[f]	0.271	32.6	6.7	21.2
C(18):C(14)PC[a]	0.324	31.2	6.6	21.0
C(18):C(14)PC[c]	0.324	29.6	5.5	17.2
C(18):C(14)PC[e]	0.324	29.9	5.8	19.8
C(18):C(14)PC[g]	0.324	29.8	5.6	19.2
C(18):C(14)PC[d]	0.324	33.0	6.0	19.6
C(18):C(14)PC[h]	0.324	31.0	6.0	19.7
C(18):C(14)PC[f]	0.324	31.4	6.3	20.7
C(12):C(20)PC[a]	0.371	25.6	4.7–5.7	15.7–19.1
C(19):C(13)PC[a]	0.417	23.8	5.0	16.8
C(11):C(21)PC[a]	0.460	32.6	9.4	30.7
C(20):C(12)PC[a]	0.500	34.5	11.5	37.4
C(20):C(12)PC[i]	0.500	33.2	11.6	37.8
C(10):C(22)PC[a]	0.538	37.8	11.9	38.3
C(10):C(22)PC[i]	0.538	37.3	12.2	39.2

[a] This work. [b] Mabrey and Sturtevant (1976). [c] Chen and Sturtevant (1981). [d] Stümpel et al. (1983). [e] Mattai et al. (1987). [f] Wang et al. (1990). [g] Huang and Mason (1986). [h] Boggs and Mason (1986). [i] Xu and Huang (1987).

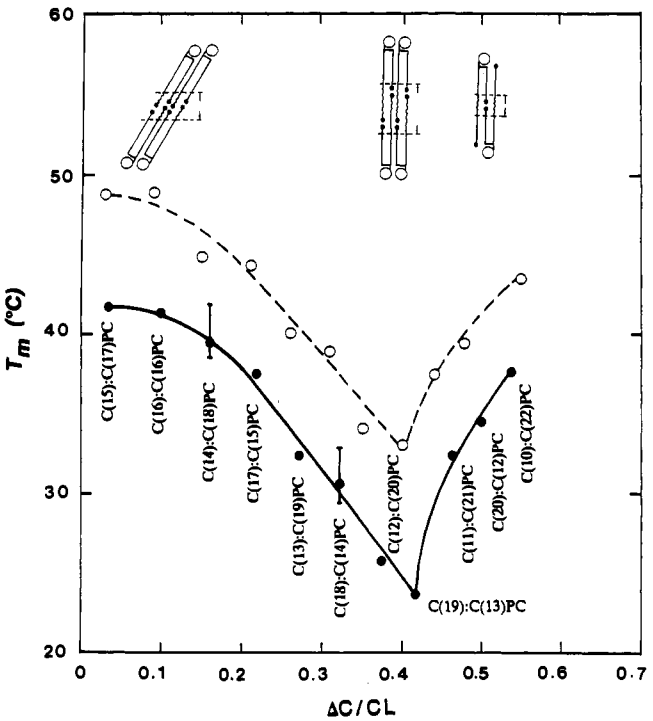

FIGURE 2: Plot of the main phase-transition temperature, T_m, versus the normalized chain length difference ($\Delta C/CL$) between the two acyl chains in various phosphatidylcholines. The solid curve connects the T_m values of liposomes prepared from the various mixed-chain phosphatidylcholines and C(16):C(16)PC as depicted in Figure 1 (solid circles). These various phospholipids have a common MW of 734.1. For comparison, the dotted curve connecting the data of Lin et al. (1990) shown in open circles for various phosphatidylcholines with a common MW of 762.1 is also drawn. Proposed models depicting the chain-end perturbations within the gel-state bilayer are diagramatically represented above each region.

smaller peak area ($\Delta H \cong 5.0$ kcal/mol), when examined in a narrower temperature range of 15–45 °C; moreover, this smaller endothermic transition is also reversible provided that the heating scan is carried out in the same temperature range of 14–45 °C. We suspect that the larger transition at 28.1 °C may be the subgel to the liquid-crystalline ($L_c \rightarrow L_\alpha$) phase transition and that the smaller transition at 25.6 °C may be the gel to liquid-crystalline phase transition. Our speculations are not totally unreasonable, since the formation of L_c phase for identical-chain phosphatidylcholines with short acyl chains has been observed to take place rather rapidly at low temperatures (Lewis et al., 1987). Clearly, additional studies are needed to confirm our speculations. In any case, the value of 25.6 °C is presented tentatively as the main phase transition temperature for C(12):C(20)PC in Table I and Figure 2.

Binary Mixtures of C(12):C(20)PC/C(16):C(16)PC. The mixing behavior of C(12):C(20)PC/C(16):C(16)PC binary mixtures was investigated calorimetrically as a function of temperature. The T_m values of aqueous dispersions prepared from these two pure phospholipids are 25.6 and 41.5 °C, respectively; these values fall on the left linear segment of the V-shaped curve in the T_m vs $\Delta C/CL$ plot as shown in Figure 2. A total of 13 representative DSC heating curves recorded in the temperature range of 15–60 °C for binary mixtures of C(12):C(20)PC/C(16):C(16)PC with indicated compositions are depicted in Figure 3A. These curves are the third DSC heating scans, after the samples have been subjected to two successive heatings (first, 5–60 °C; second, 15–60 °C) to ensure the practically identical thermal history of all the lipid dispersions.

The onset and completion temperatures of the main phase transitions exhibited by mixtures of C(12):C(20)PC/C(16):C(16)PC of 13 compositions are indicated by the solid triangles in Figure 3A. These temperatures are, in turn, plotted as a function of mol % of C(16):C(16)PC as shown in Figure 3B. The two solid curves connecting the onset and completion temperatures define the solidus and liquidus boundaries, respectively, of the phase diagram presented in Figure 3B. It should be noted that the solidus and liquidus curves in this figure do not display a point of sharp inflection or a region of horizontal line. The shape of this figure is thus typically that of an isomorphous systems, indicating that the two component lipids of all compositions form continuous solutions below and above the main phase-transition temperature (Cevc & Marsh, 1987). The two solid curves of Figure 3B delineate three regions. Binary mixtures of C(12):C(20)PC/C(16):C(16)PC of all compositions at temperatures that lie below the solidus curve are cocrystallized to form a homogeneous solutions in the gel phase (G); at temperatures above the liquidus curve the entire system is a single liquid-crytalline phase (L) of homogeneously mixed lipids; and within the solidus and liquidus curves is a two-phase region (L + G), in which domains of G and domains of L phases coexist in equilibrium. The compositions of the gel or liquid-crystalline phase in the two-phase (G + L) region can be determined from the tie line at a given temperature (Cevc & Marsh, 1987).

For the nearly ideal mixing behavior, the main phase-transition temperature of the binary mixture can be related linearly to the sum of the partial molar fraction of the T_m values for the pure component lipids. Indeed, the value of T_m for the C(12):C(20)PC/C(16):C(16)PC mixture increases linearly with increasing contents of C(16):C(16)PC as shown by the dashed line in Figure 3B. This observed linear function can thus be taken as additional evidence indicating that C-

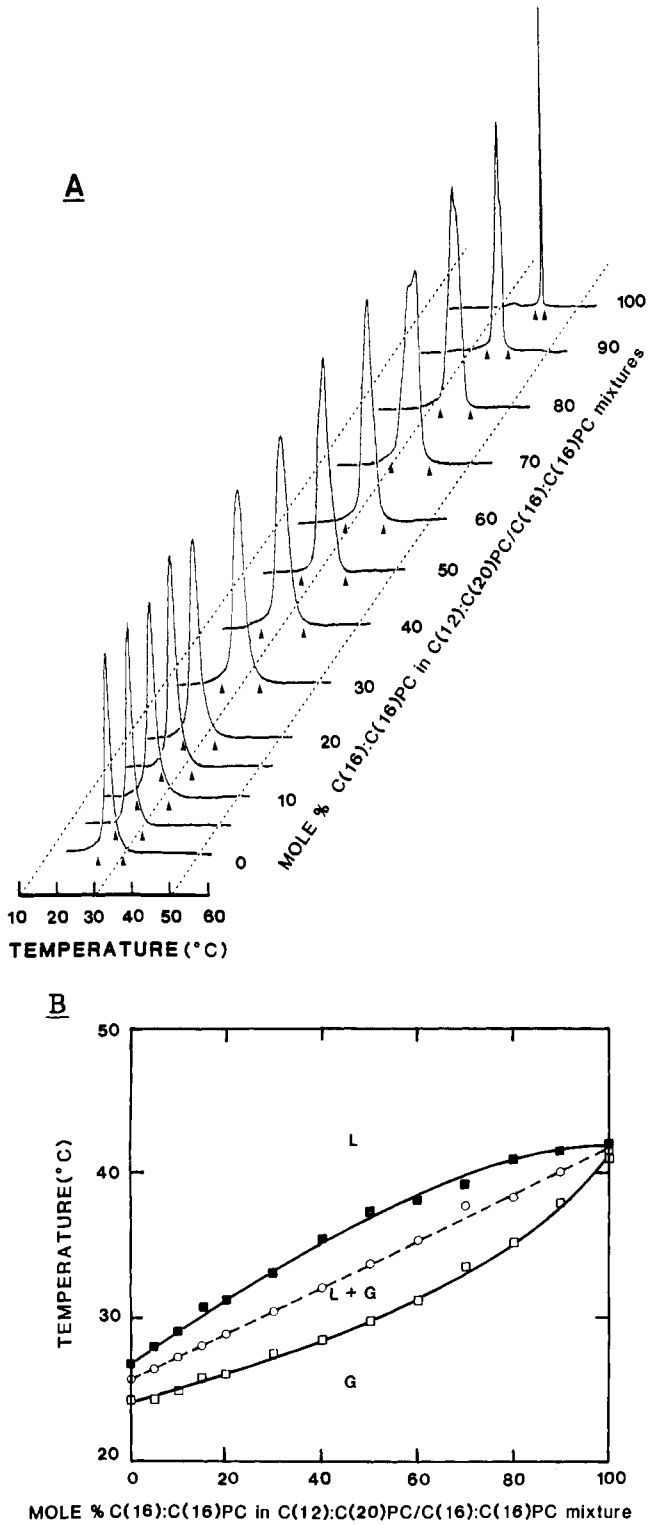

FIGURE 3: Thermal behavior of binary mixtures of C(12):C(20)-PC/C(16):C(16)PC. (A) The third DSC heating scans of C(12):C(20)PC/C(16):C(16)PC mixtures containing various mol % of C(16):C(16)PC from 15 to 55 °C at 15 °C/h. The onset and completion temperatures of the various transitions are indicated by the solid triangles. (B) Experimental phase diagram of the C(12):C-(20)PC/C(16):C(16)PC mixtures constructed on the basis of the onset (open square) and completion (solid square) temperatues of the various transitions shown in panel A. The dotted line in the two-phase (L + G) region represents the line connecting the experimental T_m values (open circles) of the various transitions shown in panel A. G and L denote the gel and liquid-crystalline phases, respectively.

(12):C(20)PC and C(16):C(16)PC are completely miscible in the gel and liquid-crystalline states. It should be pointed out that the dashed line in Figure 3B is in fact the line connecting the midpoints of all tie lines in the two-phase (G + L) region of the phase diagram. Recently, it has been shown by Vaz et al. (1990) that this line in a similar isomorphous system of binary mixtures of lipids is the thermodynamic line of connectivity. At temperatures below this line, domains of liquid-crystalline phase are disconnected and domains of gel phase are connected in the two-phase region, whereas at temperatures above this lines, domains of gel phase are disconnected but are surrounded by a continuous liquid-crystalline phase in the two-phase region.

Binary Mixtures of C(20):C(12)PC/C(10):C(22)PC. After examining the mixing behavior of C(12):C(20)PC/C(16):C-(16)PC, a pair of identical MW phospholipids with T_m values that fall on the left segment of the V-shaped curve shown in the T_m vs $\Delta C/CL$ plot (Figure 2), we carried out further DSC experiments to investigate the miscibility between C(20):C-(12)PC and C(10):C(22)PC. These two highly asymmetrical mixed-chain phospholipids with identical MW have $\Delta C/CL$ values larger than 0.420; their T_m values are shown to the far right in Figure 2.

Figure 4A illustrates the DSC heating thermograms for aqueous dispersions of C(20):C(12)PC/C(10):C(22)PC binary mixtures of 15 compositions. These DSC heating curves were scanned from 5 to 45 °C, after the samples had been subjected to two successive heating (5–45 °C) cycles in the calorimeter. As shown in Figure 4A, all lipid dispersions exhibit a single and nearly symmetrical endotherm. The highly cooperative transition of the C(20):C(12)PC dispersion at 34.8 °C shifts gradually and continuously toward higher temperatures as C(10):C(22)PC is increasingly incorporated into the C-(20):C(12)PC bilayer until the binary mixture reaches the end point at 100% C(10):C(22)PC with T_m of 40.6 °C. Similar shifts in the transition curves have been previously reported for C(22):C(12)PC/C(10):C(22)PC mixtures (Xu et al., 1987).

Onset and completion temperatures of the various transitions indicated in Figure 4A were used to map the phase diagram shown in Figure 4B. The resulting C(20):C(12)PC/C(10):C(22)PC phase diagram is very similar in shape to the C-(12):C(20)PC/C(16):C(16)PC phase diagram illustrated in Figure 3B. Specifically, the phase diagram in Figure 4B exhibits no apparent discontinuity in either the solidus or liquidus curve, indicating that these two molecular species of highly asymmetric phospholipids are completely miscible in the gel and liquid-crystalline states over the entire compositional range. In addition, the main phase-transition temperature of the binary mixture can be linearly related to the sum of the partial molar fraction of the T_m values for the pure component lipids (data not shown), again suggesting the nearly ideal mixing of the component lipids.

Binary Mixtures of C(10):C(22)PC/C(16):C(16)PC. The observed nearly ideal mixing behavior of C(12):C(20)PC/C-(16):C(16)PC and C(20):C(12)PC/C(10):C(22)PC mixtures over the entire compositional range at temperatures above and below T_m suggests strongly that in the bilayer the two component lipids in each mixing pair must have very similar structural and packing properties so that they can dissolve completely into each other in all proportions in either the gel or the liquid-crystalline state. It should be noted that the T_m (or ΔH) values of the C(12):C(20)PC/C(16):C(16)PC pair and the C(20):C(12)PC/C(10):C(22)PC pair fall on the descending and ascending segments, respectively, of the V-shaped curve in Figure 2. Thus, two phospholipids that fall on the same segment in Figure 2 may be isomorphously replaced with each other in the gel state as well as the liquid-crystalline state

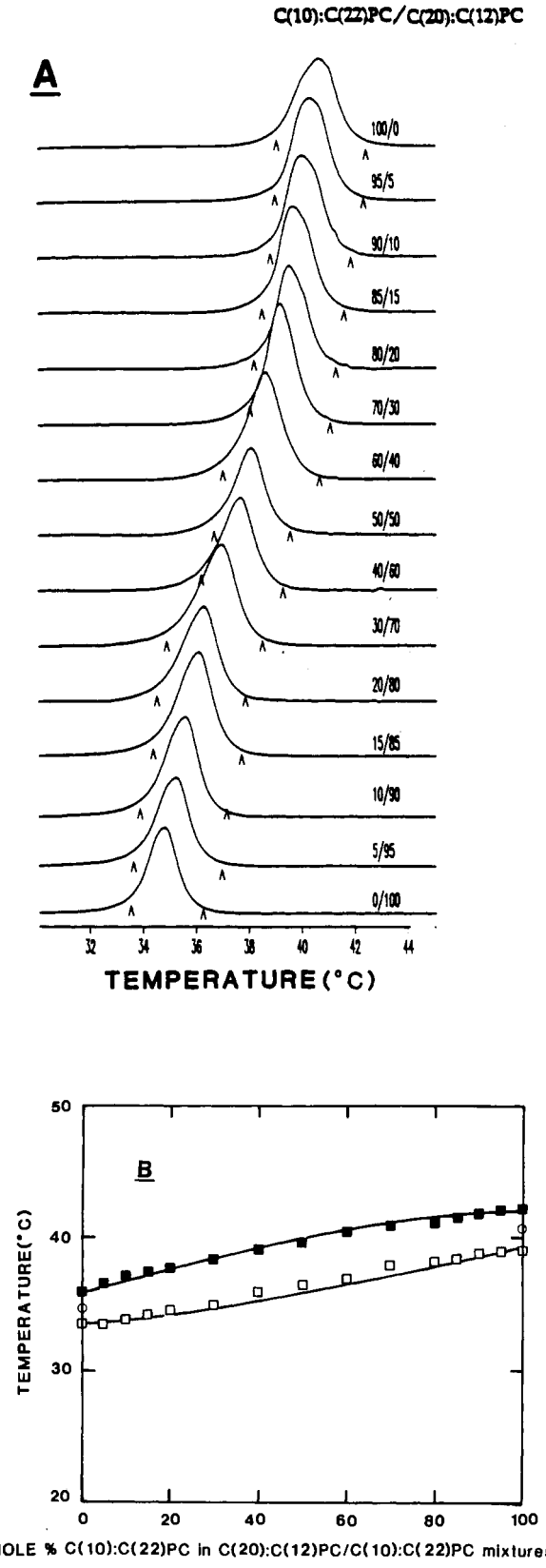

FIGURE 4: Thermal behavior of binary mixtures of C(20):C(12)-PC/C(10):C(22)PC. (A) The third DSC heating scans of C(20):C(12)PC/C(10):C(22)PC mixtures with indicated relative molar ratios of C(10):C(22)PC/C(20):C(12)PC. The onset and completion temperatures of the various main transitions, indicated by the symbol ∧, are used to map the phase diagram for C(20):C(12)PC/C-(10):C(22)PC shown in panel B. In preparing all the aqueous samples for the mixing experiments, the dry binary lipids were first co-dissolved in chloroform following the method 4 procedures of Lin and Huang (1988). This chloroform step resulted in an up-shift in T_m by about 2.8 °C for aqueous dispersions of pure C(10):C(22)PC.

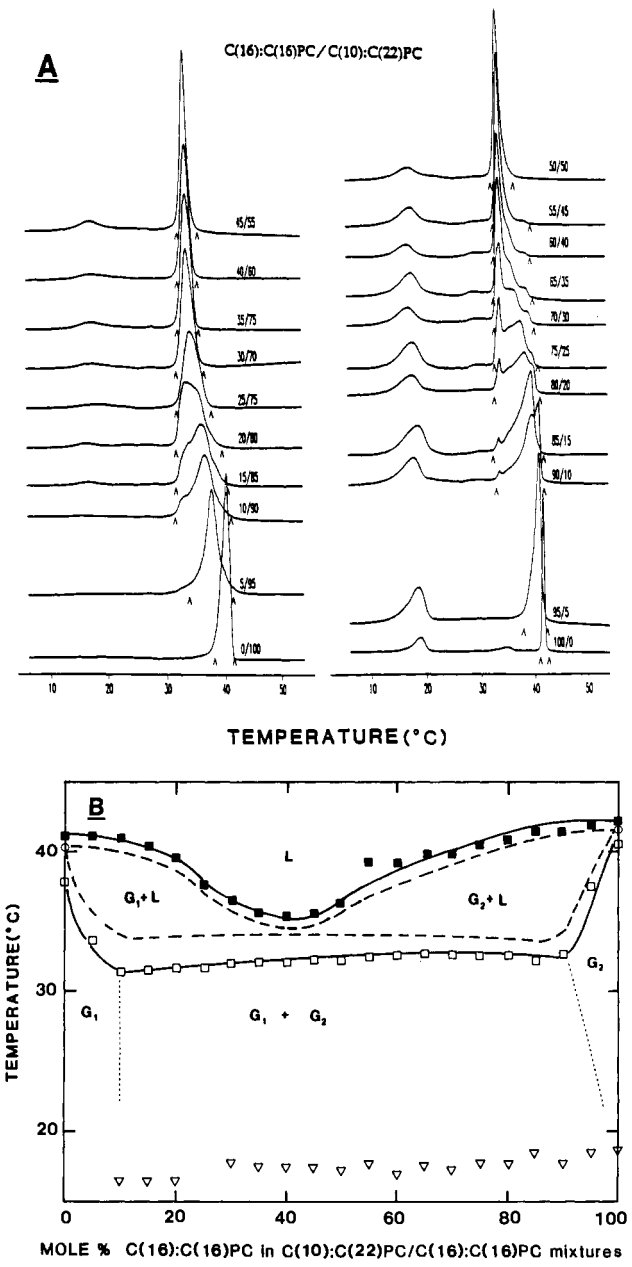

FIGURE 5: Thermal behavior of C(10):C(22)PC/C(16):C(16)PC mixtures. (A) Initial DSC heating scans of the binary mixtures with indicated molar ratios of C(16):C(16)PC/C(10):C(22)PC. (B) Solid curves indicate the boundaries of the experimental phase diagram constructed based on the onset (□) and completion (■) temperatures, respectively, of the various main phase transition peaks shown in panel A. Dashed curves define the boundaries of the phase diagram after correction for the finite width of the phase transitions of the pure components (Mabrey & Sturtevant, 1976). The symbol ▽ represents the midpoint of the subtransition. The dotted vertical lines represent the solvus lines, which are not observed by DSC but assumed.

bilayer; consequently, it raises an interesting question of whether two phospholipids identified from the two different segments of the V-shaped curve in Figure 2 are able to dissolve into each other in the bilayer at temperatures above or below T_m. To answer this question, the mixing behavior of binary mixtures of C(10):C(22)PC/C(16):C(16)PC at various temperatures was assessed by DSC.

The initial DSC heating thermograms for 21 aqueous dispersions of C(10):C(22)PC/C(16):C(16)PC mixtures of various compositions are shown in Figure 5A. The reason we present the initial DSC heating thermogram is that the broad subtransition exhibited by C(16):C(16)PC, if it exists, is dinstinctively separated from all of the main phase transitions

displayed by binary mixtures of C(10):C(22)PC/C(16):C(16)PC; hence, the broad subtransition peak does not interfere with the correct assignment of the onset temperature of the main phase transition. As shown in Figure 5A, the main phase-transition temperature of the binary mixture shifts downward from 40.4 to 34.5 °C as the C(16):C(16)PC content in the binary mixture increases steadily from 0 to 45 mol %. Between 50 and 100 mol % C(16):C(16)PC, the transition features of the main endotherm for most of C(10):C(22)PC/C(16):C(16)PC mixtures appear to be rather complex; nevertheless, the transition peak is clearly observed to shift upward in temperature from 34.7 °C at 50 mol % to 41.6 °C at 100 mol % C(16):C(16)PC.

The onset and completion temperatures of the main phase transition for this series of C(10):C(22)PC/C(16):C(16)PC mixtures are also indicated in Figure 5A and are used to map the boundaries of the phase diagram illustrated in Figure 5B. The shape of the corrected phase diagram for the C(10):C(22)PC/C(16):C(16)PC binary mixture, shown in Figure 5B, is typically that of a eutectic system (Yeh, 1990). In this system, the two component lipids are completely miscible in all proportions at temperatures above the liquidus boundary, forming a single liquid-crystalline phase designated as L phase at the top of the phase diagram. In addition, this corrected phase diagram is characterized by a long horizontal portion of the solidus boundary at 34 °C, extending approximately from 10 to 90 mol % of C(16):C(16)PC. Below this eutectic horizontal, there is a two-phase region in which domain of C(10):C(22)PC enriched gel phase (designated as G_1 phase) and domains of C(16):C(16)PC enriched gel phase (designated as G_2 phase) coexist in equilibrium. The mixtures of (G_1 + L) and (G_2 + L) make up the other two two-phase regions at the left and right, respectively, in Figure 5B. The three two-phase regions (G_1 + L, G_2 + L, and G_1 + G_2) and the one-phase L region intersect at a common point called the eutectic point. This eutectic point is the degenerated three-phase (G_1 + G_2 + L) region, corresponding to the point at 34 °C and 40 mol % of C(16):C(16)PC (Figure 5B). It should be mentioned that the eutectic phase diagram for C(10):C(22)PC/C(16):C(16)PC binary system is exceedingly similar in shape to the one previously observed for binary mixtures of C(18):C(10)PC/C(14):C(14)PC (Lin & Huang, 1988). Thus, it can be inferred that the lateral lipid–lipid interactions between the two component lipids in the two-dimensional plane of the bilayer are most likely to be very similar for these two binary lipid mixtures, each comprised of a pair of identical MW phosphatidylcholines.

Discussion

The present study described the high-resolution DSC studies of aqueous dispersions prepared from 11 different phosphatidylcholines and 3 two-component mixtures of phosphatidylcholines. These phosphatidylcholines have a common MW of 734.1, but their molecular shapes, in terms of $\Delta C/CL$, as characterized by the normalized chain length asymmetry between the two acyl chains, are quite different.

An important finding arising from this work is that any of the thermodynamic parameters (T_m, ΔH, ΔS) associated with the main phase transitions for liposomes prepared from these pure phospholipids exhibits a biphasic V-shaped curve when plotted as a function of $\Delta C/CL$. It is well known that the main phase transition of the lipid bilayer detected by DSC is an energetic event, reflecting a highly cooperative transition of the bilayer from an ordered gel state to a disordered liquid-crystalline state at T_m upon heating of the sample. The relative energetic contents and hence the relative packing modes of the lipid acyl chains between two lipid bilayer systems can thus be compared on the basis of their thermodynamic parameters association with the main phase transitions. The packing modes of lipid acyl chains can be conveniently described in terms of the conformational statistics (trans/gauche ratio) and the lateral chain–chain interactions, and they can be monitored directly by Raman spectroscopy (Levin, 1984). Comparative studies of aqueous dispersions of various identical-chain and mixed-chain phosphatidylcholines have shown that the variations in Raman order/disorder parameters for these lipids in the gel state are, in general, considerably greater than those in the liquid-crystalline state (Levin, 1984; Levin et al., 1985). Consequently, the observed changes in T_m and ΔH values associated with the main phase transitions for aqueous dispersions prepared from the various identical MW phosphatidylcholines shown in Figure 1 and Table I may be attributed primarily to the differences in the conformational statistics of the hydrocarbon chains and the lateral chain–chain van der Waals interactions of the respective phosphatidylcholines in the gel-state.

We may now interpret the biphasic curve shown in Figure 2 as follows: (1) The higher T_m (ΔH or ΔS) values for C(15):C(17)PC and C(16):C(16)PC may be indicative of relatively higher packing orders of acyl chains in these two lipid systems at $T < T_m$. The normalized chain length difference between the *sn*-1 and *sn*-2 acyl chains ($\Delta C/CL$) for these two identical MW phospholipids is very small. Moreover, this chain length heterogeneity is situated topologically in a small region near the bilayer mid-plane for both bilayer systems at $T < T_m$. The effects of $\Delta C/CL$ on the lateral packings of the rest of the lipid acyl chains and hence the cooperative melting of the rest of the linear acyl chains are likely to be minimal for these two lipid systems. (2) The thermodynamic parameters associated with the main phase transitions for various identical MW phosphatidylcholines with $\Delta C/CL$ values in the range of 0.10–0.42 are observed to decrease nearly linearly with increasing values of $\Delta C/CL$ (Figure 2 and Table I). This linear function with a negative slope implies that the conformational statistics of the hydrocarbon chains and the lateral chain–chain contact interactions of these phospholipids in the gel-state bilayer are perturbed proportionally by a progressive increase in $\Delta C/CL$. The perturbation may be attributed to the chain terminal methyl group, since the effective volume of chain terminal methyl group is more than twice that of the methylene group (Nagle & Wiener, 1988). As the value of $\Delta C/CL$ increases progressively, the overlapping regions of the terminal methyl groups of the shorter acyl chains with the adjacent upper sections of the longer acyl chains within the same leaflet and the overlapping regions of the terminal groups of the longer acyl chains with the adjacent upper sections of the longer acyl chains from the opposing leaflet become increasingly more pronounced, especially when the terminal methyl group of the short chain within the same lipid molecule comes in contact with the middle section of the longer acyl chain (Figure 2). In these overlapping regions, the bulky methyl ends are expected to distort the all-trans conformation of the adjacent methylene units in a closely packed gel-state bilayer. When the value of $\Delta C/CL$ is about 0.42, the magnitude of the perturbation may be viewed as at its maximum. Beyond this point, the highly asymmetric phosphatidylcholine in the gel-state bilayer has to adopt a new packing mode to release a certain degree of perturbations. (3) As the $\Delta C/CL$ value increases continuously in the range of 0.42–0.56, the disparity between the two acyl chains is further magnified; at the point of $\Delta C/CL = 0.5$, the longer chain is precisely twice

the effective chain length of the shorter one. We propose that these highly asymmetrical phospholipids are packed, in excess water, into the mixed interdigitated mode at $T < T_m$. In this new packing mode, the long acyl chain spans the whole width of the bilayer's hydrocarbon core, and the shorter chains, each from a lipid molecule in the opposing leaflet, meet end-to-end in the bilayer mid-plane (Huang, 1990). Such mixed interdigitated packing modes have been previously observed by X-ray diffraction techniques for C(18):C(10)PC ($\Delta C/CL$ = 0.56), C(8):C(18)PC ($\Delta C/CL$ = 0.55), C(18):C(12)PC ($\Delta C/CL$ = 0.44), and C(10):C(18)PC ($\Delta C/CL$ = 0.42) (Hui et al., 1984; McIntosh et al., 1984; Mattai et al., 1987; Shah et al., 1990). Conceivably, perturbing effects of the methyl ends can be effectively reduced in this new packing mode, since the methyl groups of the longer acyl chains are now relocated toward the two interfaces between the hydrocarbon core of the bilayer and the aqueous medium (Figure 2). This relocating feature eventually reverses the trend of the observed function in the plot of T_m (or ΔH) vs $\Delta C/CL$, thereby resulting in a biphasic V-shaped curve. The fact that C(10):C(22)PC with $\Delta C/CL$ = 0.54 has higher values of T_m, ΔH, and ΔS than C(11):C(21)PC($\Delta C/CL$ = 0.46) may be interpreted as due to the stronger lateral chain–chain contact interactions. One can readily calculate that in the case of $\Delta C/CL$ = 0.54, the sum of the effective chain length for the two shorter acyl chains plus the close van der Waals contact distance between two opposing terminal methyl groups (~2 Å) matches nearly perfectly with the effective chain length of the longer acyl chain, thus permitting the maximal lateral chain–chain van der Waals interactions for C(10):C(22)PC molecules in the mixed interdigitated bilayer.

Evidence in support of our explanations of the biphasic V-shaped curve illustrated in Figure 2 as given above can be sought in the three phase diagrams shown in Figure 3B, 4B, and 5B. The phase diagram for a binary lipid mixture provides the basic information concerning the miscibility or immiscibility of the two component lipids in the two-dimensional plane of the bilayer. The miscibility of the component lipids must depend on the lateral lipid–lipid interactions, which, in turn, depend on the structural similarity between these component lipids.

The simplest mixing behavior of a binary phospholipid system is the isomorphous system in which the two component lipids are dissolved completely into each other in both gel and liquid-crystalline states over the entire compositional range, resulting in a nearly ideal mixing behavior. Such nearly ideal mixing behavior is observed for C(12):C(20)PC/C(16):C(16)PC and C(20):C(12)PC/C(10):C(22)PC mixtures, shown in Figures 3B and 4B, respectively, and the results can be taken as evidence to indicate that a strong structural similarity exists between C(12):C(20)PC and C(16):C(16)PC and between C(20):C(12)PC and C(10):C(22)PC. If C(16):C(16)PC and C(12):C(20)PC are structurally compatible in the gel-state bilayer, then the bilayer thickness of the identical chain and of the mixed-chain phospholipids can be expected to match effectively in the gel-state bilayer (Ipsen & Mouritsen, 1988). The only packing model that permits the bilayer thickness of lipids with asymmetric chains to match well with that of identical MW C(16):C(16)PC is the one in which the longer chain of the mixed-chain phospholipid molecule on one side of the bilayer packs end-to-end with the shorter chain of another lipid molecule in the opposing bilayer leaflet at $T < T_m$. This packing model is designated as the partially interdigitated bilayer. Our proposal described earlier that the perturbing effects of chain-terminal methyl groups on the adjacent linear methylene segments of acyl chains become increasingly more pronounced as the value of $\Delta C/CL$ increases progressively from 0.10 to 0.42 is in fact based on the assumption that mixed-chain phosphatidylcholines with $\Delta C/CL$ values less than 0.42 are self-assembled, at $T < T_m$, into the partially interdigitated bilayer. Our phase diagram shown in Figure 3B indeed supports this view.

There is experimental evidence suggeting that highly asymmetric phospholipids with $\Delta C/CL$ values in the range of 0.40–0.56 including C(20):C(12)PC and C(10):C(22)PC are packed in the gel-state bilayer in a mixed interdigitated mode in excess water (Xu & Huang, 1987). This packing mode is characterized by having the area per lipid headgroup at the lipid/H_2O interface encompass three hydrocarbon chains (Huang, 1990). The observed phase diagram for C(20):C(12)PC/C(10):C(22)PC mixtures in Figure 4B suggests that the two component lipids are highly similar in the gel-state bilayer. It should be noted that these two molecular species are distinctively different in their acyl chain lengths esterified at the *sn*-1 and *sn*-2 positions of the glycerol backbone, respectively. However, if one compares either the long or the short acyl chains of these two species irrespective of their *sn* positions, the difference in acyl chain length is only about 0.5 carbon–carbon lengths. Moreover, if the difference in 0.5 C–C bonds is taken to be positive between the two long chains, then the difference between the two shorter chains is negative 0.5 C–C bonds. Nearly ideal mixing between these two lipid species in the mixed interdigitated bilayer in excess water is thus expected.

If our proposed packing model of mixed interdigitation for highly asymmetric phosphatidylcholines with $\Delta C/CL$ values in the range of 0.42–0.56 is correct, then these mixed-chain phospholipids are expected to be immiscible at $T < T_m$ with those identical MW phospholipids whose values of $\Delta C/CL$ are less than 0.42. This expectation is based on the fact that at $T < T_m$ the bilayer thickness of the mixed interdigitated bilayer is about 33% smaller than that of the partially interdigitated bilayer for phospholipids with identical MW (Hui et al., 1984; McIntosh et al., 1984). Moreover, the immiscibility is further expected to disappear at $T > T_m$, since the mixed interdigated bilayer converts to the partially interdigitated fluid phase at $T > T_m$, and, hence, the difference in the bilayer thickness becomes negligible (Hui et al., 1984; McIntosh et al., 1984).

The phase diagram shown in Figure 5B for C(10):C(22)PC/C(16):C(16)PC mixtures has the shape of a eutectic system, indicating that C(10):C(22)PC and C(16):C(16)PC are indeed immiscible at $T < 34$ °C over a wide range of composition from 10 to 90 mol % of C(16):C(16)PC and that at $T > T_m$ these two molecular species are, in contrast, completely miscible in the liquid-crystalline state. This mixing behavior is precisely the expected one on the basis of the mixed interdigitated packing mode proposed for C(10):C(22)PC.

The significance of the results presented in this work stems from several considerations. First, although the lipid bilayer has been widely viewed as an average simple-minded structure, this work shows that the equilibrium structure of the lipid bilayer is rather complex and flexible. Figure 1 clearly demonstrates that each single-component lipid bilayer comprised of phospholipids of the same family with identical MW but different $\Delta C/CL$ has its own transition characteristics; moreover, most of the lipid bilayers can undergo multiple phase transitions upon heating or cooling. Second, the structural transformation of the gel-state bilayer from the partially interdigitated mode to the mixed interdigitated mode is generally observed for phosphatidylcholines with the structural param-

eter ($\Delta C/CL$) in the range of 0.40–0.42 as shown in Figure 2. This result implies the inability of the partially interdigitated bilayer to accommodate all bulky methyl ends of the lipid acyl chains near the outer sections of the hydrocarbon core. Perturbations of these hydrocarbon sections in the phosphatidylcholine bilayer may play a role in promoting the biphasic effect of ethanol on the main phase-transition temperature of the C(16):C(16)PC bilayer. Third, the binary lipid mixtures can yield a eutectic phase diagram as depicted in Figure 5B. This finding has interesting implications in biological membranes in which the lipid acyl chains cover a wide range of different chain lengths. Near the eutectic point, the thermodynamic state of the lipid components in the two-dimensional plane of the bilayer can, under the influence of local fluctuations in either temperature or chemical composition, transform reversibly between a one-phase fluid region and a two-phase region. The dynamics and functions of a bilayer-spanning protein can thus be potentially modulated by the reversible change of the physical state of the matrix lipids in biological membranes. Hence, studies of mixed-chain phospholipids may provide basic information that is importanat in explainining the activities of integral membrane proteins (Huang, 1990).

ACKNOWLEDGMENTS

We appreciate greatly the careful reading of the manuscript and helpful comments by Dr. M. B. Sankaram. We thank Mrs. W. Harvey for typing the manuscript during the holiday season.

REFERENCES

Akiyama, M., Terayama, Y., & Matsushima, N. (1982) *Biochim. Biophys. Acta 687*, 337–338.

Boggs, J. M., & Mason, T. J. (1986) *Biochim. Biophys. Acta 863*, 231–242.

Cevc, G. and Marsh, D. (1987) *Phospholipid Bilayers. Physical Principles and Models*, Chapter 13, pp 369–406, Wiley-Interscience, New York.

Chapman, D., Williams, R. M., & Ladbrooke, B. D. (1967) *Chem. Phys. Lipids 1*, 445–475.

Chen, S. C., & Sturtevant, J. M. (1981) *Biochemistry 20*, 713–718.

Chen, S. C., Sturtevant, J. M., & Gaffney, B. J. (1980) *Proc. Natl. Acad. Sci. U.S.A. 77*, 5060–5063.

Cho, K. C., Choy, C. L., & Young, K. (1981) *Biochim. Biophys. Acta 663*, 14–21.

Chong, P. L.-G., & Choate, D. (1989) *Biophys. J. 55*, 551–556.

Huang, C. (1990) *Klin. Worchenschr. 68*, 149–165.

Huang, C. (1991) *Biochemistry 30*, 26–30.

Huang, C., & Mason, J. T. (1986) *Biochim. Biophys. Acta 864*, 423–470.

Hui, S. W., Mason, J. T., & Huang, C. (1984) *Biochemistry 23*, 5570–5577.

Ipsen, J. H., & Mouritsen, O. G. (1988) *Biochim. Biophys. Acta 944*, 121–134.

Lentz, B. R., Freire, E., & Biltonen, R. L. (1978) *Biochemistry 17*, 4475–4480.

Levin, I. W. (1984) *Adv. Infrared Raman Spectrosc. 11*, 1–48.

Levin, I. W., Thompson, T. E., Bareholz, Y., & Huang, C. (1985) *Biochemistry 24*, 6282–8286.

Lewis, R. N. A. H., Mark, N., & McElhaney, R. N. (1987) *Biochemistry 26*, 6118–6126.

Lin, H.-n., & Huang, C. (1988) *Biochim. Biophys. Acta 946*, 178–184.

Lin, H.-n., Wang, Z-q., & Huang, C. (1990) *Biochemistry 29*, 7063–7072.

Mabrey, S., & Sturtevant, J. M. (1976) *Proc. Natl. Acad. Sci., U.S.A. 73*, 3862–3866.

Mason, J. T., Huang, C., & Biltonen, R. L. (1981) *Biochemistry 20*, 6086–6092.

Mattai, J., Sripada, P. K., & Shipley, G. G. (1987) *Biochemistry 26*, 3287–3297.

McIntosh, T. J., Simon, S. A., Ellington, J. C., & Porter, N. A. (1984) *Biochemistry 23*, 4038–4044.

Nagle, J. F., & Wiener, M. C. (1988) *Biochim. Biophys. Acta 942*, 1–10.

Nambi, P., Rowe, E., & McIntosh, T. J. (1988) *Biochemistry 27*, 9175–9182.

Ohki, K., Tamura, K., & Hatta, I. (1990) *Biochim. Biophys. Acta 1028*, 215–222.

Rowe, E. S. (1983) *Biochemistry 22*, 3299–3305.

Ruocco, M. I., & Shipley, G. G. (1982) *Biochim. Biophys. Acta 691*, 309–320.

Shah, J., Scripada, P. K., & Shipley, G. G. (1990) *Biochemistry 29*, 4254–4262.

Simon, S. A., & McIntosh, T. J. (1984) *Biochim. Biophys. Acta 773*, 169–172.

Simon, S. A., McIntosh, T. J., & Hines, M. L. (1986) in *Molecular and Cellular Mechanisms of Anesthetics* (Roth, S. H., & Miller, K. W. Eds.) pp 279–318, Plenum, New York.

Sisk, R. B., Wang, Z.-q., Lin, H-n., & Huang, C. (1990) *Biophys. J. 58*, 777–783.

Slater, J. L., & Huang, C. (1988) *Prog. Lipid Res. 27*, 325–359.

Stümpel, T., Eibl, H., & Nicksch. A. (1983) *Biochim. Biophys. Acta 727*, 246–264.

Vaz, W. L. C., Melo, E. C. C., & Thompson, T. E. (1990) *Biophys. J. 58*, 273–275.

Wang, Z-q., Lin, H-n., & Huang, C. (1990) *Biochemistry 29*, 7072–7076.

Wu, W., Chong, P. L.-G., & Huang, C. (1985) *Biophys. J. 47*, 237–242.

Xu, H., & Huang, C. (1987) *Biochemistry 26*, 1036–1043.

Xu, H., Stephenson, F. A., & Huang, C. (1987) *Biochemistry 26*, 5448–5453.

Yeagle, P. (1987) *The Membranes of Cells*, pp 22–61, Academic Press, New York.

Yeh, H. C. (1970) in *Phase Diagrams: Materials Science and Technology* (Alper, A. M., Ed.) Vol. 1, pp 167–197, Academic Press, New York.